annalen der physik
www.ann-phys.org

Optical Nonreciprocity in Rotating Diamond with Nitrogen-Vacancy Color Centers

*Hong-Bo Huang, Jun-Jie Lin, Yi-Xuan Yao, Ke-Yu Xia, Zhang-Qi Yin, and Qing Ai**

A method to realize optical nonreciprocity in rotating nano-diamond with nitrogen-vacancy (NV) centers is theoretically proposed here. Because of the relative motion of the NV center with respect to the propagating fields, the frequencies of the fields are shifted due to the Doppler effect. When the control and probe fields are incident to the NV center from the same direction, the two-photon resonance still holds as the Doppler shifts of the two fields are the same. Thus, due to the electromagnetically-induced transparency, the probe light can pass through the NV center nearly without absorption. However, when the two fields propagate in opposite directions, the probe light cannot effectively pass through the NV center as a result of the breakdown of two-photon resonance.

1. Introduction

Optical nonreciprocity happens when Lorentz's reciprocity is broken, and it leads to different transmittances when two beams of light propagate in the opposite directions.[1] Optical nonreciprocity plays an important role in optical devices such as isolators and circulators,[2] which have further application in quantum networks,[3,4] quantum noise reduction,[5] quantum signal processing,[6,7] and photon blockade.[8–10] Traditional nonreciprocity is mainly realized by magneto-optical effect,[11–13] which often requires such large size that it is difficult to be used on chips. To overcome this shortcoming, alternative strategies are explored to achieve nonreciprocity, including nonlinear optics,[14–16] synthetic magnetism,[11,17,18] optomechanical coupling,[19–21] and nontrivial topology.[22] Interestingly, it has been shown that nonreciprocal transport can also be realized by the irregular thermal motion of atoms.[23–26]

In 1961, Fano pointed out that if several different atomic transitions are coupled, the total transition probability will be coherently enhanced or cancelled due to the interference of the amplitudes of these transitions.[27] Inspired by this discovery, many studies on atomic coherence appeared, for example, electromagnetically-induced transparency (EIT).[28] In EIT, adding a strong control field can make the medium transparent for the probe light, which will be resonantly absorbed by the atomic medium in the absence of the control field.[29] Because it has a wide range of prospective applications, for example, nonreciprocal transmission and memory of nonclassical fields,[30,31] EIT has been successfully realized in many systems, such as gas-phase atoms,[32,33] photosynthetic energy transfer,[34,35] metamaterial,[36] superconducting system,[37] and NV center in diamond.[38]

On the other hand, nitrogen-vacancy (NV) center in diamond is an intriguing platform for quantum information processing[39–41] and quantum sensing.[42,43] NV center is a pair of point defects at adjacent sites in diamond crystal. Due to long coherence time and easy manipulation at room temperature, it has been shown that it can be utilized for detecting magnetic cluster,[44] state transfer by shortcut to adiabaticity,[45–47] gyroscope,[48,49] and quantum hyperbolic metamaterial.[50] Recently, it has been experimentally realized that nanoparticles levitated in vacuum can rotate at a frequency of GHz.[51–53] Inspired by the rapid progress on the quantum coherent devices by NV centers, a question naturally comes to our mind: Can we make use of a rotating diamond with NV centers for realizing optical nonreciprocity?

In this paper, we propose a non-reciprocal transmission based on a rotating nano-diamond at a high speed. The nano-diamond doped with NV centers is placed in an optical cavity. Two electronic ground states and one electronic excited state of the NV center form a Λ-type three-level configuration and the optical transitions between the ground states the excited state can be induced by electromagnetic fields, that is, the control field and the cavity field. We explore the transmittance of the probe light incident in different directions with respect to the control field.

H.-B. Huang, J.-J. Lin, Y.-X. Yao, Q. Ai
Department of Physics
Applied Optics Beijing Area Major Laboratory
Beijing Normal University
Beijing 100875, China
E-mail: aiqing@bnu.edu.cn

K.-Y. Xia
National Laboratory of Solid State Microstructures
Collaborative Innovation Center of Advanced Microstructures
College of Engineering and Applied Sciences and School of Physics
Nanjing University
Nanjing 210093, China

Z.-Q. Yin
Center for Quantum Technology Research and Key Laboratory of Advanced Optoelectronic Quantum Architecture and Measurements (MOE)
School of Physics
Beijing Institute of Technology
Beijing 100081, China

The ORCID identification number(s) for the author(s) of this article can be found under https://doi.org/10.1002/andp.202200157

DOI: 10.1002/andp.202200157

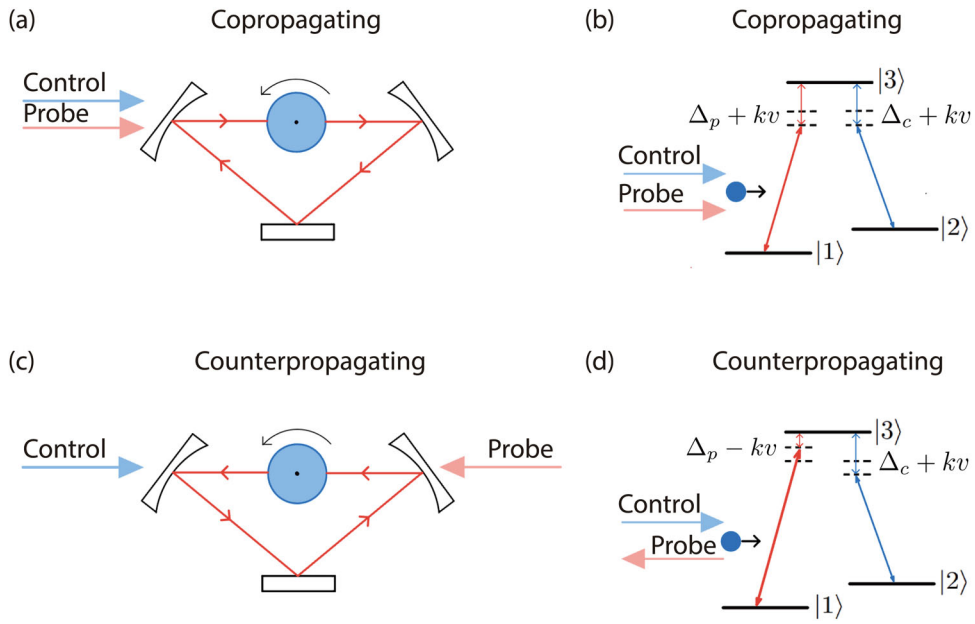

Figure 1. Schematic diagram of optical nonreciprocity in a rotating nano-diamond with the NV centers. (a) and (c) are the cases when the probe and the control field propagate in the same/opposite direction, respectively. A high-speed rotating nano-diamond is placed in an optical cavity. After the lights entering the cavity, they are coupled with the NV centers in the nano-diamond. b,d) Energy-level diagrams for (a,c), respectively. Due to the relative motion between the NV centers and the lights, different Doppler shifts are induced. When the laser and the NV centers move along the same direction, the Doppler shift is $\Delta + kv$. Otherwise, the Doppler shift is $\Delta - kv$.

The paper is organized as follows: In Section 2, we first introduce the model of the system and we derive the expressions of the transmittance at the steady state by the Heisenberg–Langevin approach. In Section 3, we numerically show the transmittances for the two cases and analyze the results by the dark-state mechanism in ref. [38]. Finally, we discuss the prospect of our proposal and summarize the main findings in Section 4.

2. Theoretical Model

We consider a rapidly-rotating nano-diamond with NV centers in an optical cavity, as illustrated in **Figure 1**. The control light and the probe light respectively interact with the optical transitions at $\lambda = 637.2$ nm of the NV center from the electronic ground state $|\pm 1\rangle$ to the electronic excited state $|A_2\rangle$.[45,50] The cavity mode with resonance frequency ω_a is coupled to the transition $|1\rangle(\equiv |+1\rangle) \leftrightarrow |3\rangle(\equiv |A_2\rangle)$ with Rabi frequency g. Moreover, there is a beam of probe laser injected into the cavity. A strong control laser beam with a carrier frequency ω_c and Rabi frequency Ω_c is coupled to the transition $|2\rangle(\equiv |-1\rangle) \leftrightarrow |3\rangle$.

The relative motion between a single NV center and photons gives rise to the microscopic Doppler shift, that is, $\omega_\alpha - \vec{k}_\alpha \cdot \vec{v}$. Here, ω_α $(\alpha = a, c)$ is the frequency of the photons experienced by the NV center when the latter is at rest. $\vec{k}_\alpha$ is the wave vector of the light in the nano-diamond and $\vec{v}$ is the velocity of the NV center. For example, if the NV center and the light move in the same direction, the frequency of the photon experienced by the NV center becomes $\omega_\alpha - k_\alpha v$.

Assuming $\hbar = 1$, the Hamiltonian of the system takes the following form

$$
\begin{aligned}
H = {} & \omega_a a^\dagger a + \omega_p a_p^\dagger a_p + \sum_{l=1}^{3} \omega_l \sigma_{ll} + \sum_r \omega_r d_r^\dagger d_r \\
& + \sum_q \omega_q b_q^\dagger b_q + \Omega_c e^{i(\omega_c - \vec{k}_c \cdot \vec{v})t} \sigma_{23} + g e^{-i\vec{k}_a \cdot \vec{v} t} a^\dagger \sigma_{13} \\
& + i\sqrt{\kappa_1} a^\dagger a_p + \sum_r g_r d_r^\dagger a + \sum_q (g_{1q}\sigma_{31} + g_{2q}\sigma_{32}) b_q \\
& + \text{h.c.} \qquad (1)
\end{aligned}
$$

where ω_l $(l = 1, 2, 3)$ is the energy of state $|l\rangle$, and $\hat{\sigma}_{lm} = |l\rangle\langle m|$ is the operator of NV center, a $(a^\dagger)$ and a_p $(a_p^\dagger)$ are respectively the annihilation (creation) operators of the cavity mode and the probe field, Ω_c is the Rabi frequency of the control field with frequency ω_c and wave vector $\vec{k}_c$, g is the Rabi frequency of the cavity mode with frequency ω_a and wave vector $\vec{k}_a$. b_q $(b_q^\dagger)$ and d_r $(d_r^\dagger)$ are annihilation (creation) operators of the reservoirs interacting with the NV center and the cavity mode respectively, where ω_q and ω_r are the frequencies of the corresponding harmonic oscillators. g_r, g_{1q}, and g_{2q} correspond to the coupling strength between the reservoirs and the cavity mode, atomic transition $|1\rangle \leftrightarrow |3\rangle$, and $|2\rangle \leftrightarrow |3\rangle$, respectively. Strictly speaking, there should be a factor $\exp(-i\vec{k} \cdot \vec{r})$ in the coupling constant g. However, since we assume the radius of the nano-diamond is $r_n = 63.7$ nm, which

is much smaller than the wavelength of the light, this factor is reasonably neglected.

By using the unitary transformation

$$U = \exp\{i[\omega_p a^\dagger a + \omega_p a_p^\dagger a_p + \sum_r \omega_r d_r^\dagger d_r + \sum_q \omega_q b_q^\dagger b_q + (\omega_3 - \omega_p + \vec{k}_a \cdot \vec{v})\sigma_{11} + (\omega_3 - \omega_c + \vec{k}_c \cdot \vec{v})\sigma_{22} + \omega_3 \sigma_{33}]t\} \quad (2)$$

we can obtain the effective Hamiltonian in the rotating frame as

$$H_I = \Delta_a a^\dagger a + (\Delta_p + \vec{k}_a \cdot \vec{v})\sigma_{11} + (\Delta_c + \vec{k}_c \cdot \vec{v})\sigma_{22} + \Omega_c \sigma_{32} + g a^\dagger \sigma_{13} + i\sqrt{\kappa_1} a^\dagger a_p + \sum_q (g_{1q}\sigma_{31} e^{i(\omega_p - \vec{k}_a \cdot \vec{v} - \omega_q)t} + g_{2q}\sigma_{32} e^{i(\omega_c - \vec{k}_c \cdot \vec{v} - \omega_q)t}) b_q + \sum_r g_r d_r^\dagger a e^{i(\omega_r - \omega_p + \vec{k}_a \cdot \vec{v})t} + \text{h.c.} \quad (3)$$

where $\Delta_a = \omega_a - \omega_p$ represents the detuning between the cavity mode and the probe laser, $\Delta_p = \omega_3 - \omega_1 - \omega_p$ is the detuning between the probe laser and the transition $|1\rangle \leftrightarrow |3\rangle$, and $\Delta_c = \omega_3 - \omega_2 - \omega_c$ is the detuning between the control laser and the transition $|2\rangle \leftrightarrow |3\rangle$.

Among the methods for open quantum systems,[54,55,59] the Heisenberg–Langevin approach can faithfully reproduce the quantum dynamics. Especially, it can significantly-reduce the complexity of calculation as compared to the widely used quantum master equation[60,61] and numerically-exact hierarchical equation of motion,[62–65] when the system under investigation contains bosons and the number of operators of interest is relatively small. In order to obtain the transmittance of the probe light, we apply the Heisenberg–Langevin approach to obtain

$$\dot{a} = -i(\Delta_a + \frac{\kappa}{2})a + \sqrt{\kappa_1} a_p - i g \sigma_{13} + F_a \quad (4)$$

$$\dot{\sigma}_{13} = -[\gamma_3 + i(\Delta_p + \vec{k}_a \cdot \vec{v})]\sigma_{13} - i\Omega_c \sigma_{12} + i g a(\sigma_{33} - \sigma_{11}) + F_3 \quad (5)$$

$$\dot{\sigma}_{12} = -[\gamma_{12} - i(\Delta_p + \vec{k}_a \cdot \vec{v}) + i(\Delta_c + \vec{k}_c \cdot \vec{v})]\sigma_{12} - i\Omega_c \sigma_{13} + i g a \sigma_{32} + F_2 \quad (6)$$

where $\kappa = \kappa_1 + \kappa_2 + \kappa_c$, κ_1 (κ_2) is the coupling rate for the input (output) of the probe laser, and κ_c is the intrinsic damping rate of cavity, γ_3 is the spontaneous decay rate associated with the electronic excited state $|3\rangle$, and γ_{12} is the dephasing rate between the two ground states $|1\rangle$ and $|2\rangle$. F_a, F_3, and F_2 are the Langevin noise operators of a, σ_{13}, and σ_{12}, respectively, which arise through the interaction with the reservoir, that is,

$$F_a = -i\sum_r g_r d_r(0) e^{-i(\omega_r - \omega_p)t} \quad (7)$$

$$F_3 = i\sum_q [g_{1q}(\sigma_{33} - \sigma_{11}) b_q(0) e^{-i(\omega_q - \omega_p + \vec{k}_a \cdot \vec{v})t} - g_{2q}\sigma_{12} b_q(0) e^{-i(\omega_q - \omega_c + \vec{k}_c \cdot \vec{v})t}] \quad (8)$$

$$F_2 = i\sum_q [g_{1q}\sigma_{32} b_q(0) e^{-i(\omega_q - \omega_p + \vec{k}_a \cdot \vec{v})t} - g_{2q}\sigma_{13} b_q(0) e^{-i(\omega_q - \omega_c + \vec{k}_c \cdot \vec{v})t}] \quad (9)$$

Generally speaking, because the NV centers in nano-diamond interact with a complicated bath of phonons and spins, γ_3 and γ_{12} show dependence on various factors, for example, the temperature, the magnetic field, and the density of magnetic impurities.[66] By generalization of cluster correlation expansion, we can numerically simulate the open quantum dynamics of the NV center in the presence of spin bath at the low temperature.[67,68]

The initial state of NV center is prepared at $|1\rangle$ by optical pumping.[45] Next, we consider the steady-state solution by setting $\langle \dot{a} \rangle = 0$, $\langle \dot{\sigma}_{13} \rangle = 0$, and $\langle \dot{\sigma}_{12} \rangle = 0$. In our configuration with $g \ll \Omega_c$, we have $\langle \sigma_{11} \rangle \approx 1$ and $\langle \sigma_{32} \rangle \approx 0$. Within the mean-field approximation, we have $\langle F_a \rangle = \langle F_3 \rangle = \langle F_2 \rangle = 0$. By setting $\Delta_a = \Delta_c = 0$ and solving Equations (4–6), we can obtain

$$\langle a \rangle_\pm = \frac{\sqrt{\kappa_1}\langle a_p \rangle}{i\Delta_p + \kappa/2 + i\chi_\pm} \quad (10)$$

$$\chi_\pm = \frac{-i|g|^2}{\gamma_3 + i(\Delta_p + k_a v) + \frac{|\Omega_c|^2}{\gamma_{12} + i[\Delta_p + (k_a \mp k_c)v]}} \quad (11)$$

where χ is the susceptibility of the NV center to the cavity mode, the subscript + (−) corresponds to the co-propagation (counter-propagation) case. Due to the mutual movement of NV center and light, the Doppler effect cannot be ignored. In our system, the control laser is always injected from the left side, while the probe laser can propagate in either the same or the opposite direction. As shown in Figure 1, we shall only consider the component of the velocity which is parallel to the direction of light propagation for the Doppler effect. Therefore, as shown in Figure 1a,c, assuming that both the control and probe fields are of the same wave length, we have $\vec{k}_c \cdot \vec{v} = kv$ for both cases, while $\vec{k}_a \cdot \vec{v} = kv$ for the co-propagation and $\vec{k}_a \cdot \vec{v} = -kv$ for the counter-propagation, respectively.

According to the input–output theory,[54,55] the amplitude of the output field of the cavity is $\sqrt{\kappa_2}\langle a \rangle_+$ ($\sqrt{\kappa_1}\langle a \rangle_-$) in the co-propagation (counter-propagation) case. Thus, the transmission spectra for the co-propagation (counter-propagation) case T_+ (T_-) can be written as[55]

$$T_\pm = \left| \frac{\sqrt{\kappa_1 \kappa_2}}{i\Delta_p + \kappa/2 + i\chi_\pm} \right|^2 \quad (12)$$

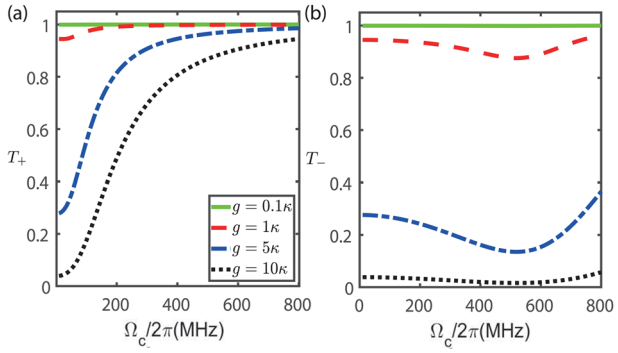

Figure 2. The transmittance versus the Rabi frequency Ω_c of the control field for the probe light in the a) co-propagation and b) counter-propagation cases, respectively. The green solid line refers to the case with $g = 0.1\kappa$, the red dashed line for $g = \kappa$, the blue dash-dotted line for $g = 5\kappa$, and the black dotted line for $g = 10\kappa$. The parameters are $v = 250$ m s^{-1}, $\Delta_a = \Delta_p = 0$, $\kappa_1 = 2\pi \times 0.5$ MHz, $\kappa_2 = 2\pi \times 4$ MHz, $\kappa_c = 2\pi \times 6$ MHz,[25] $\gamma_{12} = 2\pi \times 8.8$ MHz,[45] $\gamma_3 = 1809.3$ MHz at $T_n = 30$ K.[56] Due to the heat absorbed from the laser, the temperature of composite nano-particle is increased from $T_e = 5.5$ K to $T_n = 30$ K, where we have used the cooling scheme proposed in ref. [57].

By the contrast of the two transmittance defined as[69]

$$\eta = \frac{T_+ - T_-}{T_+ + T_-} \tag{13}$$

we can evaluate the nonreciprocity of the rotating NV center.

3. Numerical Results and Analysis

We consider the nonreciprocal transport at the steady state. As shown in **Figure 2**a for the co-propagation case with $v = 250$ m s^{-1}, for example, a nano-diamond rotating at 4 GHz with an NV center located at radius 62.5 nm from the spin axis, we find a nearly-unity transport when $g \gg \kappa$ and Ω_c is large enough. This result demonstrates that the probe light explores the dark state for lossless transmission. In contrast, when the probe light propagates in the opposite direction of the control light, there is a fall around $\Omega_c = 500$ MHz. This fall becomes profounder when g is increased. Due to the term $2kv$ in χ_- of Equation (11), χ_- should achieve a maximum value at some Ω_c.

In order to investigate the underlying physical mechanism for the nonreciprocal transport, we explore the dark-state mechanism in ref. [38]. The time evolution of the wave function is written as

$$|\psi(t)\rangle = -\frac{\Omega_c}{\Omega} e^{-i\frac{g^2}{\Omega^2}\omega_2 t}|E_1\rangle + \frac{g}{\sqrt{2}\Omega} e^{-\frac{i}{2}(\omega_1 + \frac{\Omega_c^2}{\Omega^2}\omega_2)t}(e^{-i\Omega t}|E_2\rangle + e^{i\Omega t}|E_3\rangle) \tag{14}$$

where $\Omega = \sqrt{g^2 + \Omega_c^2}$, $|E_j\rangle$'s are the three eigen states of the non-Hermitian system with $|E_1\rangle$ being the dark state and $|E_{2,3}\rangle$ being the bright states, $\omega_1 = \delta - i\gamma_3$ with δ being single-photon detuning, $\omega_2 = \Delta - i\gamma_{12}$ with Δ being two-photon detuning. The explicit expressions of the three eigen states are given as

$$|E_1\rangle \simeq \frac{1}{N_1}[(\omega_1\omega_2 - \Omega_c^2)|1\rangle - g\omega_2|3\rangle + g\Omega_c|2\rangle] \tag{15}$$

$$|E_2\rangle \simeq \frac{1}{N_2}\{[(\Omega - \omega_1)(\Omega - \omega_2) - \Omega_c^2]|1\rangle + g(\Omega - \omega_2)|3\rangle + g\Omega_c|2\rangle\} \tag{16}$$

$$|E_3\rangle \simeq \frac{1}{N_3}\{[(\Omega + \omega_1)(\Omega + \omega_2) - \Omega_c^2]|1\rangle - g(\Omega + \omega_2)|3\rangle + g\Omega_c|2\rangle\} \tag{17}$$

with N_i's being the normalization constants.

In our proposal, when the NV center is at rest, we set two-photon resonance for the control and probe fields, that is, $\Delta = 0$. When the NV center rotates along with the nano-diamond, the Doppler shifts will arise for the two fields. In the co-propagating case, since the Doppler shifts will be the same, the two-photon resonance still holds. When $g \ll \Omega_c$, cf. **Figure 3**a,b, the probe field is immune to absorption because the dark state dominates, that is, $\Omega_c/\Omega \simeq 1$, in the wave function, which decays at a lower rate of $(g^2/\Omega^2)\gamma_{12}$. If g is increased, cf. Figure 3c,d, two factors will enhance the absorption. On the one hand, because $\omega_1\omega_2 - \Omega_c^2 \ll g\omega_2, g\Omega_c$, $|2\rangle$ and $|3\rangle$ play a more significant role in $|E_1\rangle$. It makes the dark state more lossy, since it will decay at a larger rate as g is increased. On the other, the two bright states will make a greater contribution, about $g/\sqrt{2}\Omega$, to $|\psi(t)\rangle$ with a faster decay rate $(\gamma_3 + \kappa/2 + \Omega_c^2\gamma_{12}/\Omega^2)/2$. Therefore, we can observe a wider region for low transmittance as we increase g in Figure 3a–d.

If we turn to the counter-propagation case, we can observe a more interesting dependence of transmittance on v and Ω_c. When $g \ll \kappa$, as shown in Figure 3e, the transmittance is almost kept at unity for the whole parameter region. However, when $g = \kappa$ in Figure 3f, there emerges a dip in the transmittance for $kv = \sqrt{2}\Omega_c$. Along this line, we have $\omega_1\omega_2 - \Omega_c^2 \simeq 2(kv)^2 - \Omega_c^2 = 0$ and thus there is no component of $|1\rangle$ in $|E_1\rangle$. The main contribution from $|E_2\rangle$ and $|E_3\rangle$ in $|\psi(t)\rangle$ results in the lossy transmission. As g increases, this area of exception becomes wider. Interestingly, the width of the dip is almost not influenced by either v or Ω_c, but g. According to our numerical simulation as shown in **Figure 4**, the velocity corresponding to the full width at half maximum (FWHM) of the contrast is proportional to g^2.

In the above discussion, we only consider a single NV center. However, because the absorption cross section of a single NV center may be poor,[58] we shall improve the light–matter interaction by using an ensemble of NV centers, which we often encounter in practice. Hereafter, we will consider a ball-shaped diamond with radius r_n, containing N NV centers and rotating at an angular velocity ω. We assume that the light's propagating along the x-axis and the diamond is rotating along the y-axis. In this case, we have $\vec{\omega} = \omega\vec{j}$ and the NV center is instantly located at $\vec{r} = x\vec{i} + y\vec{j} + z\vec{k}$. The linear velocity of the NV center along the direction of light's propagation reads

$$v_x = (\vec{\omega} \times \vec{r}) \cdot \vec{i} = \omega z \tag{18}$$

Since the velocity of the NV center along the light's direction depends only on its coordinate along z-axis, we can convert its distribution of velocity into the distribution of position along the

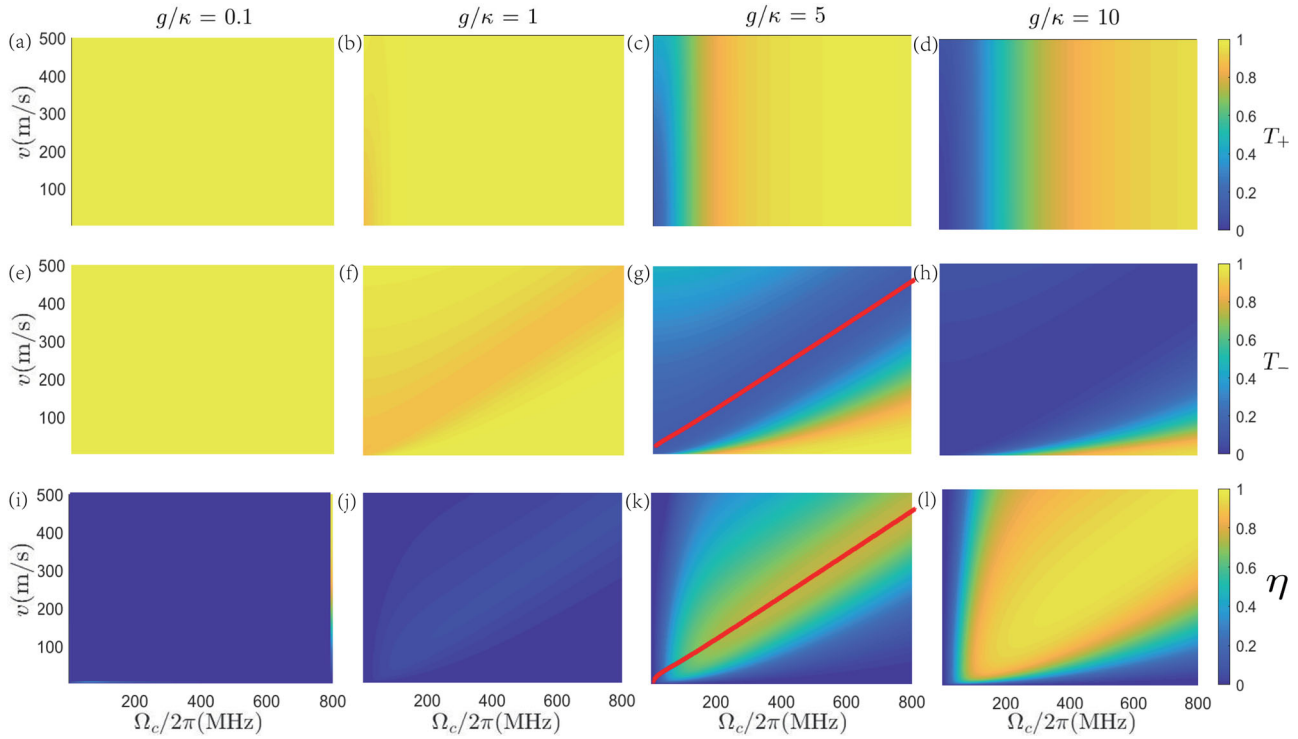

Figure 3. The relationship between the transmittance, T_+ (T_-) contrast, η the control field strength Ω_c and the velocity v. a– h) The top (middle) row corresponds to the transmittance T_+ (T_-) in the co-propagation (counter-propagation) case. i– l) The bottom row shows the contrast η. From left to right, each column corresponds to $g/\kappa = 0.1,\ 1,\ 5,$ and 10, respectively. The red lines in (g) and (k) is the minimum value located at $kv = \Omega_c/\sqrt{2}$. All numerical simulations are based on the same parameters as Figure 2.

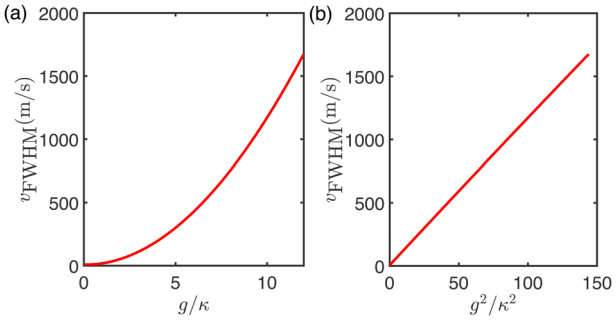

Figure 4. The velocity v_{FWHM} for the FWHM of η versus a) g and b) g^2 in Figure 3. Obviously, v_{FWHM} is proportional to g^2.

z-axis, by using $v = \omega z$ and $dv = \omega dz$, and thus obtain

$$D_v(v)\mathrm{d}v = D_v(\omega z)\omega \mathrm{d}z = D_z(z)\mathrm{d}z \tag{19}$$

where

$$D_z(z) = \frac{1}{N}\int_{-\sqrt{r_n^2-z^2}}^{\sqrt{r_n^2-z^2}}\int_{-\sqrt{r_n^2-y^2-z^2}}^{\sqrt{r_n^2-y^2-z^2}} n\mathrm{d}x\mathrm{d}y$$
$$= \frac{3}{4r_n^3}(r_n^2 - z^2) \tag{20}$$

Here, we have used $n = 3N/(4\pi r_n^3)$ as the density of NV centers in the diamond. And we can obtain

$$D_v(v) = \frac{1}{\omega}D_z(\frac{v}{\omega}) = \frac{3}{4(\omega r_n)^3}[(\omega r_n)^2 - v^2] \tag{21}$$

On account of NV centers with different linear velocities, we replace Equation (11) by

$$\chi'_{\pm} = \int_{-\omega r_n}^{\omega r_n} N\chi_{\pm}(v)D_v(v)\mathrm{d}v \tag{22}$$

The numerical simulations are correspondingly shown in **Figure 5**. It can be seen that there still exists the non-reciprocal transmission although the integration is performed in the range $(-\omega r_n, \omega r_n)$. That is because the two-photon resonance, as required by the EIT, still holds as along the probe light and control light propagate in the same direction no matter the velocity is positive or not. In this case, the term $(k_a - k_c)v$ will cancel in the denominator of χ_+, cf. Equation (11). As a result, it leads to the sharp contrast between T_+ and T_- and thus the non-reciprocal transmission. In other words, the appearance of EIT phenomenon does not depend on the sign of the Doppler shift, but whether the Doppler shifts of the two beams are the same or not. We can see that the non-reciprocal transmission occurs only when ω reaches above $k\omega r_n = \sqrt{2}\Omega_c$. The area of the non-reciprocity grows as $\sqrt{N}g$ becomes larger and larger as compared to κ.

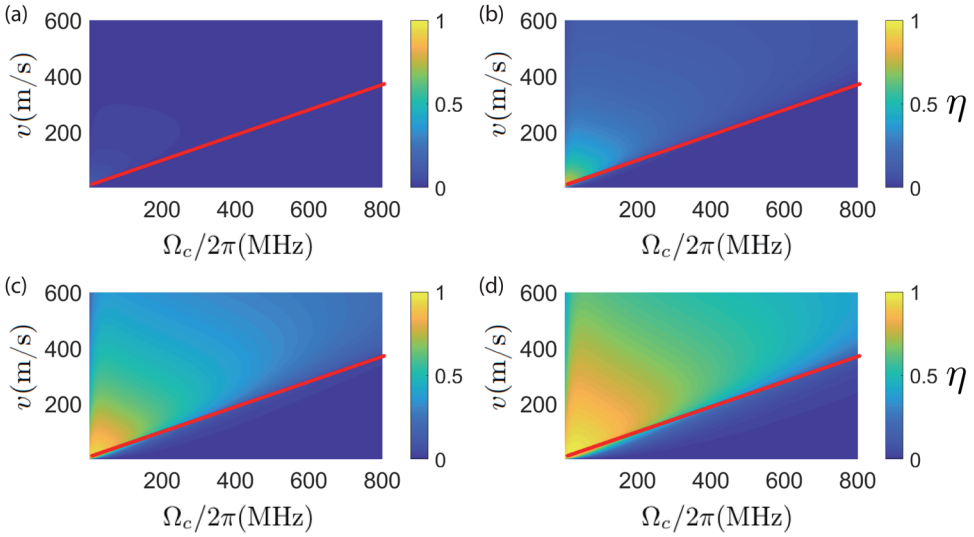

Figure 5. The relationship between the contrast η, the Rabi frequency of the control field Ω_c and the angular velocity ω. From (a) to (d), $\sqrt{N}g/\kappa$ = 0.1, 1, 5, and 10. The red lines correspond to $k\omega r_n = \Omega_c/\sqrt{2}$, above which the non-reciprocal transmission starts to appear.

In order to effectively observe the non-reciprocity, we need to separate the coherently-scattered light from the incoherently-scattered light by phonon sideband. According to ref. [58], the wavelength of the incoherently-scattered light is above 650 nm, while that of the coherently-scattered light remains unchanged, that is, 637 nm. Therefore, by setting the resonant frequency of the cavity at 637 nm, we can effectively separate these two scattered lights because the cavity plays the role as a narrow-band filter in ref. [58].

In practice, optically-trapped nano-diamonds with NV centers might absorb the energy of laser beams in an optical tweezer. The high-vacuum environment, which is employed to increase the speed of the rotating nano-diamond, might make the dissipation of the absorbed heat more difficult. However, in order to overcome this problem, we employ a nano-diamond coated with a less-absorptive silica shell optically-trapped in the azimuthally-polarized Gaussian beam and the linearly-polarized Laguerre–Gaussian beam LG_{03}.[57] Because the cross-section intensity distribution of the doughnut beam has a dark region at the beam center, the heat absorption will be significantly suppressed when the dark region of the beam coincides with the diamond core. In **Figure 6**, by using the numerical-simulation approach in ref. [57], we show the temperature of the composite particle due to the heating by the laser beams. When the temperature of the high-vacuum environment is $T_e = 5.5$ K, the temperature of the composite particle will be kept lower than $T_n = 30$ K as long as the power of the incident laser is smaller than 400 mW, which is much larger than $P_{inc} = 100$ mW for trapping a nano-particle with $R = 1$ μm.[57]

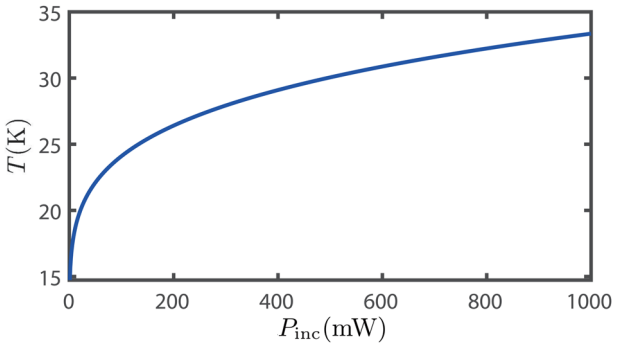

Figure 6. The temperature of the composite particle versus the power of the laser beam P_{inc} due to heat absorption. The temperature of the high-vacuum environment is $T_e = 5.5$ K, and the radius of the nano-particle is $R = 1$ μm. We employ a nano-diamond coated with a less-absorptive silica shell optically-trapped in the azimuthally-polarized Gaussian beam and the linearly-polarized Laguerre–Gaussian beam LG_{03}.[57]

4. Conclusion and Discussion

In this paper, we explore the nonreciprocal transport in rotating nano-diamond induced by the EIT and the Doppler shift. We obtain the results at the steady state by the Heisenberg–Langevin approach. It is shown that the probe light makes use of the dark state and its transmission is generally not affected by the lossy intermediate state when it is incident in the same direction of the control light. However, the transmittance is significantly depressed around $kv = \Omega_c/\sqrt{2}$ due to the breakdown of the two-photon resonance when the probe and control lights are in the opposite direction. Thus, we propose realizing optical nonreciprocity by using rotating nano-diamond with NV centers. We also discover that the velocity of the FWHM of the transmission contrast is proportional to g^2.

Previously, it was experimentally shown that the energies of the electronic ground states of NV centers in diamond will be shifted due to the rotation as a result of Barnett effect.[70–73] However, since the energies of the electronic excited states will be correspondingly shifted by the same amount, the energy spectra in Figure 1 will not be modified by the rotation. Thus, the above

proposed nonreciprocal transmission in rotating nano-diamond with NV centers still holds.

Acknowledgements

H.-B.H., J.-J.L., and Y.-X.Y. contributed equally to this work. The authors thank stimulating discussions with Lei-Ming Zhou, Jie-Qiao Liao, Jian Lin, and Yu-Qiao Li. This work was supported by the National Natural Science Foundation of China under Grant Nos. 11674033, 11474026, 11505007, Beijing Natural Science Foundation under Grant No. 1202017, and Beijing Normal University under Grant No. 2022129.

Conflict of Interest

The authors declare no conflict of interest.

Data Availability Statement

The data that support the findings of this study are available from the corresponding author upon reasonable request.

Keywords

electromagnetically induced transparency, nitrogen-vacancy centers, optical nonreciprocity

Received: April 9, 2022
Revised: June 21, 2022
Published online: August 3, 2022

[1] M. Born, E. Wolf, *Principles of Optics*, Cambridge University Press, Cambridge **1999**.
[2] D. Jalas, A. Petrov, M. Eich, W. Freude, S. Fan, Z. F. Yu, R. Baets, M. Popovic, A. Melloni, A. D. Joannopoulos, M. Vanwolleghem, C. R. Doerr, H. Renner, *Nat. Photonics* **2013**, *7*, 579.
[3] H. Kimble, *Nature (London)* **2008**, *453*, 1023.
[4] P. Lodahl, S. Mahmoodian, S. Stobbe, P. Schneeweiss, J. Volz, A. Rauschenbeutel, H. Pichler, P. Zoller, *Nature (London)* **2017**, *541*, 473.
[5] Y. Shoji, T. Mizumoto, H. Yokoi, I. W. Hsieh, R. M. Osgood Jr, *Appl. Phys. Lett.* **2008**, *92*, 071117.
[6] A. B. Khanikaev, A. Alù, *Nat. Photonics* **2015**, *9*, 359.
[7] Z. F. Yu, S. H. Fan, *Nat. Photonics* **2009**, *3*, 91.
[8] S. Maayani, R. Dahan, Y. Kligerman, E. Moses, A. U. Hassan, H. Jing, F. Nori, D. N. Christodoulides, T. Carmon, *Nature (London)* **2018**, *558*, 569.
[9] R. Huang, A. Miranowicz, J.-Q. Liao, F. Nori, H. Jing, *Phys. Rev. Lett.* **2018**, *121*, 153601.
[10] J. F. Huang, Q. Ai, Y. G. Deng, C. P. Sun, F. Nori, *Phys. Rev. A* **2012**, *85*, 023801.
[11] L. D. Tzuang, K. Feng, P. Nussenzveig, S. Fan, M. Lipson, *Nat. Photonics* **2014**, *8*, 701.
[12] A. B. Khanikaev, S. H. Mousavi, G. Shvets, Y. S. Kivshar, *Phys. Rev. Lett.* **2010**, *105*, 126804.
[13] L. Bi, J. Hu, P. Jiang, D. H. Kim, G. F. Dionne, L. C. Kimerling, C. A. Ross, *Nat. Photonics* **2011**, *5*, 758.
[14] N. Bender, S. Factor, J. D. Bodyfelt, H. Ramezani, D. N. Christodoulides, F. M. Ellis, T. Kottos, *Phys. Rev. Lett.* **2013**, *110*, 234101.
[15] L. Fan, J. Wang, L. T. Varghese, H. Shen, B. Niu, Y. Xuan, A. M. Weiner, M. Qi, *Science* **2012**, *335*, 447.
[16] L. Chang, X. Jiang, S. Hua, C. Yang, J. Wen, L. Jiang, G. Li, G. Wang, M. Xiao, *Nat. Photonics* **2014**, *8*, 524.
[17] K. Fang, Z. Yu, S. Fan, *Nat. Photonics* **2012**, *6*, 782.
[18] K. Fang, Z. Yu, S. Fan, *Phys. Rev. Lett.* **2012**, *108*, 153901.
[19] F. Ruesink, M. A. Miri, A. Alù, E. Verhagen, *Nat. Commun.* **2016**, *7*, 13662.
[20] X. W. Xu, Y. Li, *Phys. Rev. A* **2015**, *91*, 053854.
[21] X. W. Xu, L. N. Song, Q. Zheng, Z. H. Wang, Y. Li, *Phys. Rev. A* **2018**, *98*, 063845.
[22] H.-Y. Zhu, X.-Y. Hu, J.-J. Lin, J.-Y. Wu, S. Li, Y.-X. Wang, F.-G. Deng, N.-N. Zhang, *Ann. Phys. (Berlin, Ger.)* **2021**, *533*, 2100297.
[23] C. Liang, B. Liu, A. N. Xu, X. Wen, C. C. Lu, K. Y. Xia, M. K. Tey, Y. C. Liu, L. You, *Phys. Rev. Lett.* **2020**, *125*, 123901.
[24] M. X. Dong, K. Y. Xia, W. H. Zhang, Y. C. Yu, Y. H. Ye, E. Z. Li, L. Zeng, D. S. Ding, B. S. Shi, G. C. Guo, F. Nori, *Sci. Adv.* **2021**, *7*, eabe8924.
[25] S. C. Zhang, Y. Q. Hu, G. W. Lin, Y. P. Niu, K. Y. Xia, J. B. Gong, S. Q. Gong, *Nat. Photonics* **2018**, *12*, 744.
[26] G. W. Lin, S. C. Zhang, Y. Q. Hu, Y. P. Niu, J. B. Gong, S. Q. Gong, *Phys. Rev. Lett.* **2019**, *123*, 033902.
[27] U. Fano, *Phys. Rev.* **1961**, *124*, 1866.
[28] S. E. Harris, J. E. Field, A. Imamoglu, *Phys. Rev. Lett.* **1990**, *64*, 1107.
[29] M. O. Scully, M. S. Zubairy, *Quantum Optics*, Cambridge University Press, England **1997**.
[30] M. Lobino, C. Kupchak, E. Figueroa, A. I. Lvovsky, *Phys. Rev. Lett.* **2009**, *102*, 203601.
[31] K. Honda, D. Akamatsu, M. Arikawa, Y. Yokoi, K. Akiba, S. Nagatsuka, T. Tanimura, A. Furusawa, M. Kozuma, *Phys. Rev. Lett.* **2008**, *100*, 093601.
[32] A. M. Akulshin, S. Barreiro, A. Lezama, *Phys. Rev. A* **1998**, *57*, 2996.
[33] M. Mücke, E. Figueroa, J. Bochmann, C. Hahn, K. Murr, S. Ritter, C. J. Villas-Boas, G. Rempe, *Nature (London)* **2010**, *465*, 755.
[34] H. Dong, D. Z. Xu, J. F. Huang, C. P. Sun, *Light: Sci. Appl.* **2012**, *1*, e2.
[35] L. Xu, Z.-R. Gong, M.-J. Tao, Q. Ai, *Phys. Rev. E* **2018**, *97*, 042124.
[36] N. Papasimakis, V. A. Fedotov, N. I. Zheludev, S. L. Prosvirnin, *Phys. Rev. Lett.* **2008**, *101*, 253903.
[37] P. M. Anisimov, J. P. Dowling, B. C. Sanders, *Phys. Rev. Lett.* **2011**, *107*, 163604.
[38] Y.-Y. Wang, J. Qiu, Y.-Q. Chu, M. Zhang, J.-M. Cai, Q. Ai, F.-G. Deng, *Phys. Rev. A* **2018**, *97*, 042313.
[39] H. J. Zhang, X. Y. Chen, Z.-Q. Yin, *Adv. Quantum Technol.* **2021**, *4*, 2000154.
[40] M. W. Doherty, N. B. Manson, P. Delaney, F. Jelezko, J. Wrachtrup, L. C. L. Hollenberg, *Phys. Rep.* **2013**, *528*, 1.
[41] M.-J. Tao, M. Hua, Q. Ai, F.-G. Deng, *Phys. Rev. A* **2015**, *91*, 062325.
[42] R. Schirhagl, K. Chang, M. Loretz, C. L. Degen, *Annu. Rev. Phys. Chem.* **2014**, *65*, 83.
[43] L. S. Li, H. H. Li, L. L. Zhou, Z. S. Yang, Q. Ai, *Acta. Phys. Sin.* **2017**, *66*, 230601.
[44] N. Zhao, J.-L. Hu, S.-W. Ho, J. T. K. Wan, R. B. Liu, *Nat. Nanotechnol.* **2011**, *6*, 242.
[45] B. B. Zhou, A. Baksic, H. Ribeiro, C. G. Yale, F. J. Heremans, P. C. Jerger, A. Auer, G. Burkard, A. A. Clerk, D. D. Awschalom, *Nat. Phys.* **2017**, *13*, 330.
[46] X. K. Song, Q. Ai, J. Qiu, F. G. Deng, *Phys. Rev. A* **2016**, *93*, 052324.
[47] X.-K. Song, H. Zhang, Q. Ai, J. Qiu, F.-G. Deng, *New J. Phys.* **2016**, *18*, 023001.
[48] M. P. Ledbetter, K. Jensen, R. Fischer, A. Jarmola, D. Budker, *Phys. Rev. A* **2012**, *86*, 052116.
[49] A. Ajoy, P. Cappellaro, *Phys. Rev. A* **2012**, *86*, 062104.
[50] Q. Ai, P.-B. Li, W. Qin, J.-X. Zhao, C. P. Sun, F. Nori, *Phys. Rev. B* **2021**, *104*, 014109.

[51] R. Reimann, M. Doderer, E. Hebestreit, R. Diehl, M. Frimmer, *Phys. Rev. Lett.* **2018**, *121*, 033602.
[52] J. H. Ahn, Z. J. Xu, J. H. Bang, Y.-H. Deng, T. M. Hoang, Q. K. Han, R.-M. Ma, T. C. Li, *Phys. Rev. Lett.* **2018**, *121*, 033603.
[53] T. M. Hoang, Y. Ma, J. H. Ahn, J. H. Bang, F. Robicheaux, Z.-Q. Yin, T. C. Li, *Phys. Rev. Lett.* **2016**, *117*, 123604.
[54] C. W. Gardiner, *Quantum Noise*, Springer, Berlin **1991**.
[55] D. F. Walls, G. J. Milburn, *Quantum Optics*, Springer-Verlag, Berlin **1994**.
[56] K.-M. C. Fu, C. Santori, P. E. Barclay, L. J. Rogers, N. B. Manson, R. G. Beausoleil, *Phys. Rev. Lett.* **2009**, *103*, 256404.
[57] L.-M. Zhou, K.-W. Xiao, J. Chen, N. Zhao, *Laser Photonics Rev.* **2017**, *11*, 1600284.
[58] T. H. Tran, P. Siyushev, J. Wrachtrup, I. Gerhardt, *Phys. Rev. A* **2017**, *95*, 053831.
[59] M.-J. Tao, N.-N. Zhang, P.-Y. Wen, F.-G. Deng, Q. Ai, G.-L. Long, *Sci. Bull.* **2020**, *65*, 318.
[60] H.-P. Breuer, F. Petruccione, *The Theory of Open Quantum Systems*, Oxford University Press, Oxford **2007**.
[61] Q. Ai, Y.-J. Fan, B.-Y. Jin, Y.-C. Cheng, *New J. Phys.* **2014**, *16*, 053033.
[62] A. Ishizaki, G. R. Fleming, *J. Chem. Phys.* **2009**, *130*, 234111.
[63] B.-X. Wang, M.-J. Tao, Q. Ai, T. Xin, N. Lambert, D. Ruan, Y.-C. Cheng, F. Nori, F.-G. Deng, G.-L. Long, *npj Quantum Inf.* **2018**, *4*, 52.
[64] N.-N. Zhang, M.-J. Tao, W.-T. He, F.-G. Deng, N. Lambert, Q. Ai, *Front. Phys.* **2021**, *16*, 51501.
[65] X.-Y. Chen, N.-N. Zhang, W.-T. He, X.-Y. Kong, M.-J. Tao, F.-G. Deng, Q. Ai, G.-L. Long, *npj Quantum Inf.* **2022**, *8*, 22.
[66] A. Jarmola, V. M. Acosta, K. Jensen, S. Chemerisov, D. Budker, *Phys. Rev. Lett.* **2012**, *108*, 197601.
[67] N. Zhao, S. W. Ho, R. B. Liu, *Phys. Rev. B* **2012**, *85*, 115303.
[68] Z. S. Yang, Y. X. Wang, M. J. Tao, W. Yang, M. Zhang, Q. Ai, F. G. Deng, *Ann. Phys. (N. Y., NY, U. S.)* **2020**, *413*, 168063.
[69] D. W. Wang, H. T. Zhou, M. J. Guo, J. X. Zhang, S. Y. Zhu, *Phys. Rev. Lett.* **2013**, *110*, 093901.
[70] S. J. Barnett, *Phys. Rev.* **2009**, *6*, 239.
[71] S. J. Barnett, *Rev. Mod. Phys.* **1935**, *7*, 129.
[72] A. A. Wood, E. Lilette, Y. Y. Fein, V. S. Perunicic, L. C. L. Hollenberg, R. E. Scholten, A. M. Martin, *Nat. Phys.* **2017**, *13*, 1070.
[73] X.-Y. Chen, T. C. Li, Z.-Q. Yin, *Sci. Bull.* **2019**, *64*, 380.